PAGEOPH, Vol. 131, Nos. 1/2 (1989) 0033-4553/89/020043-18$1.50 + 0.20/0

The Fractal Geometry of Interfaces and the Multifractal Distribution of Dissipation in Fully Turbulent Flows

K. R. SREENIVASAN,[1] R. R. PRASAD,[1] C. MENEVEAU,[1] and R. RAMSHANKAR[1,2]

Abstract—We describe scalar interfaces in turbulent flows *via* elementary notions from fractal geometry. It is shown by measurement that these interfaces possess a fractal dimension of 2.35 ± 0.05 in a variety of flows, and it is demonstrated that the uniqueness of this number is a consequence of the physical principle of Reynolds number similarity. Also, the spatial distribution of scalar and energy dissipation in physical space is shown to be multifractal. We compare the $f(\alpha)$ curves obtained from one- and two-dimensional cuts in several flows, and examine their value in describing features of turbulence in the three-dimensional physical space.

Key words: Fractals, multifractals, turbulent flows, interfaces, energy and scalar dissipation.

1. Introduction

One can define a variety of surfaces in turbulent flows. Some examples are the vorticity interface (that is, the conceptual surface separating domains of intense and zero vorticity fluctuations), iso-concentration surfaces (in reacting or nonreacting flows), iso-velocity surfaces, and iso-dissipation surfaces. A common property of these surfaces is that they are highly convoluted at many scales, and possess many shapes. Their complexity defeats attempts to describe them by means of classical geometry. MANDELBROT (in many papers and his 1982 book) has advanced the necessary framework for describing the geometry of such complex shapes; he also recognized that the self-similarity expected to hold in turbulence (according to the conventional wisdom succinctly described by RICHARDSON's (1922) rhyme) could permit fractal description of such surfaces. In Section 2 we demonstrate, using as an example the particular case of scalar surfaces (that is, surfaces marking the boundary of the scalar-marked regions in a turbulent flow), that the expectation is indeed valid. We also show in Section 3 that the experimentally measured value

[1] Mason Laboratory, Yale University, New Haven, CT 06520, U.S.A.
[2] Present Address: Department of Physics, Haverford College, Haverford, PA 19041, U.S.A.

of the fractal dimension can be deduced from the principle of Reynolds number similarity (that is, negligible dependence on viscosity of global properties such as the overall growth rates of turbulent flows). In Section 4, we summarize our earlier results regarding the multifractal distribution of dissipation, and interpret these results in the light of the more general multifractal formalism recently proposed by MANDELBROT (1988).

This paper overlaps with our earlier work (SREENIVASAN and MENEVEAU, 1986; MENEVEAU and SREENIVASAN, 1987a; SREENIVASAN *et al.*, 1989; PRASAD *et al.*, 1988—referred to respectively as I, II, III and IV below), but differs from those publications in two respects. First, some aspects related to different orientations of the intersecting planes used to measure fractal dimensions, dependence on thresholds, scaling ranges, etc., are described more fully here; some additional data on turbulent wakes are also provided. A second feature is that we revisit the interpretation of the observed multifractal features of turbulence obtained by low-dimensional intersections.

2. *Experiments and Results on the Geometry of Interfaces*

Figure 1 shows a thin longitudinal slice along the axis of a turbulent jet of water emerging from a well-contoured nozzle of circular cross-section into a tank of still water. The jet was made visible by mixing a small amount (of the order of 10 parts per million) of a fluorescing dye (sodium fluorescein) into the nozzle fluid, and exciting fluorescence by illuminating a thin section of the flow by a sheet of light. Care was taken to ensure that the fluorescence was not saturated. The light source was a pulsed Nd:YAG laser with a pulse width of about 8 ns (small enough to freeze the motion), and power density of up to 2×10^7 Js^{-1} per pulse; the light sheet had a thickness of the order of 200–250 μm, which is on the order of the estimated Kolmogorov scale (that is, the smallest *dynamical* scale in the flow). Not resolved here are even smaller scales in the dye concentration fluctuations, expected to occur because of the large Schmidt number, Sc, of the dye. (Schmidt number is the ratio of the kinematic viscosity ν of the fluid to the mass diffusivity of the scalar; in the present experiments its value is of the order of 10^3.) It is legitimate to consider the plane intersection "mathematically thin" with respect to scales of the order of the Kolmogorov scale and larger. The visualized region, extending from 8 to 24 nozzle diameters downstream of the nozzle, was imaged on to a CCD camera with a 1300 (vertical) $\times$ 1000 (horizontal) pixel array, yielding a pixel resolution on the order of 150 μm^2. Further processing was done on a VAX station II/GPX.

The image shows a number of geometrically interesting features, one of which relates to the boundary that separates the nozzle fluid from the ambient tank fluid. The boundary is convoluted on a variety of scales, and appears to be disconnected at many places. It is possible that some out-of-plane connections may exist and that

Figure 1
A thin axial section of the nozzle fluid in an axisymmetric turbulent jet marked by a fluorescing dye. The nozzle Reynolds number is 4000.

the boundary is indeed connected; to establish this aspect properly, at least several simultaneous sections would be needed. Such measurements have now been completed and will be reported separately. In any case, one can imagine in three-dimensional space a surface that separates the nozzle fluid from the ambient tank fluid, a surface whose section by a plane is seen in Figure 1. This surface is of interest to us for many reasons, the primary one being that its geometry (which itself is a consequence of some dynamical constraints) will bear some relation to the amount and nature of mixing that occurs between the nozzle and tank fluids. For example, if the tank fluid were slightly acidic and the jet fluid slightly alkaline, the surface geometry will govern the amount and distribution of the product formed as a result of the reaction between the acid and the base.

As mentioned earlier, our objective is to characterize this surface (and in general all surfaces of interest in turbulent flows) by fractals; a primary property of a fractal surface being its fractal dimension, we want to measure it. We shall obtain the fractal dimension of the boundary seen in Figure 1, and later examine the sense

in which it relates to the fractal dimension of the surface embedded in three dimensions.

The first step is to specify how the boundary can be defined for further processing. Complex algorithms can be developed for the purpose, but we have shown elsewhere (see I and, PRASAD and SREENIVASAN, 1989) that it is adequate to use simple criteria based on the brightness threshold in the image (which is directly proportional to the concentration threshold on the nozzle fluid). Figure 2 shows the computer-drawn boundary obtained by setting the threshold at a brightness level that seems more or less satisfactory. One can now apply one of several techniques (described, for example, in Mandelbrot's book) to determine the fractal dimension of the boundary so marked. We have used both the box-counting and codimension methods. The codimension method was described in detail in I. In the box-counting methods, also briefly described in I, we cover the whole plane of

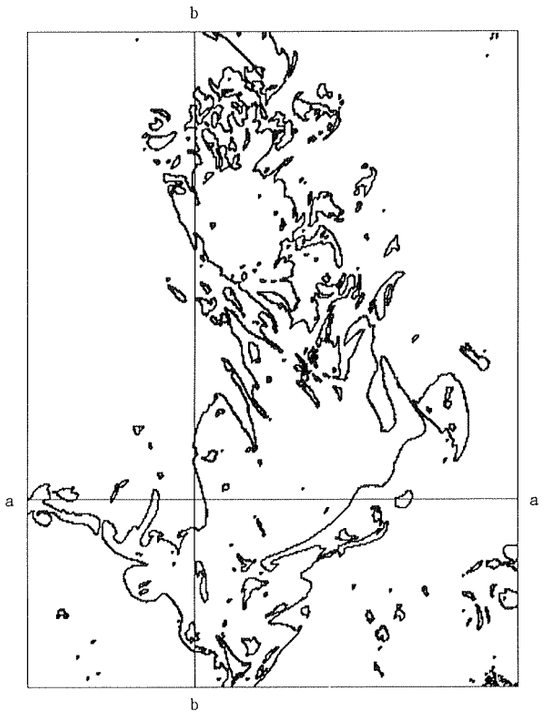

Figure 2
The boundary of the jet cross-section given in Figure 1, determined by prescribing a threshold on brightness (proportional to the concentration of the nozzle fluid). Also shown are typical (horizontal $(a-a)$ and vertical $(b-b)$) line intersections through the boundary; these will be discussed later in the text.

Figure 2 with square area elements of varying sizes, and count only the fraction $N(r)$ of elements containing the boundary, and plot log $N(r)$ as a function of logarithm of the 'box' size r; if the boundary is a fractal, we should expect an extensive straight part in this log-log plot, whose negative slope is the fractal dimension. A typical result (Figure 3a) shows that this is indeed the case, the straight part extending from the smallest scale resolved here to approximately a scale of the order of the nozzle diameter, giving a fractal dimension of 1.35 for the boundary. (It is worth mentioning that the computer programs for obtaining fractal dimensions have been checked extensively on several mathematically generated fractal sets of known dimension.)

Some minor ambiguities exist in defining the interface merely by means of a threshold, and so measurements have been repeated for several thresholds on a number of realizations of the jet. Figure 3b shows a plot of these results. It is clear that there exists a wide range of threshold values over which the fractal dimension of the boundary is essentially independent of the threshold, and that the mean value is 1.35. The spread of the data around this mean value is roughly in the range ± 0.05. Figure 3c shows that the range of scale of similarity (that is, the range of scales over which the log-log plot has a straight part) varies somewhat with threshold, but is generally about 1.5 to 2 decades. This is approximately the ratio of the large scale L to the Kolmogorov scale η in the flow.

Similar experiments in various other flows have been conducted, and Figure 4 shows an axial section of the turbulent wake of a circular cylinder. The scalar boundary in each case was marked in a similar way, and fractal dimension was computed as before. The principal results are summarized in Table 1. All measurements were made by slicing flows with the plane of light sheet along the preferred direction of each flow. Without attaching significance to minor variations from one flow to another, we may conclude that a mean value is about 1.35. It would be useful, for later discussion, to take flow slices in different orientations. A typical result from such measurements is given in Figure 5 for the mixing layer between two streams of equal and opposite directions (RAMSHANKAR, 1988). It is seen that the boundaries of the flow in two orthogonal intersections possess the same fractal dimension. This conclusion also holds for all other flows investigated here.

We may now ask how the fractal dimension from planar intersections is related to the fractal dimension D of the surface itself—this being our major concern. This general problem has been discussed in the literature, and some specific results are available for special cases (see MARSTRAND, 1954, whose results have been generalized by MATTILA, 1975). The equivalent result in the present context, as stated by MANDELBROT (1982, p. 366), relates to the additive properties of codimensions of intersections. Specifically, if S_1 and S_2 are two *independent* sets embedded in a space of dimension d, *and* if codimension (S_1) + codimension $(S_2) < d$, the codimension of $S_1 \cap S_2$ is equal to the sum of the codimensions of S_1 and S_2. For a fractal set F embedded in three-dimensional space and intersected by

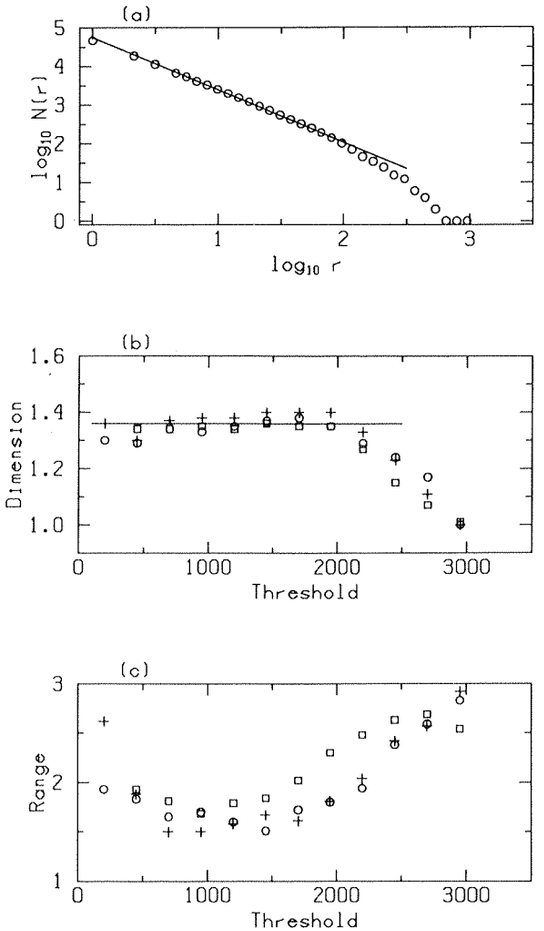

Figure 3
(a) The log-log plot of the number $N(r)$ of the area elements ('boxes') of size r containing the interface. The negative slope of the straight part gives the fractal dimension of the boundary (= 1.35). The abscissa ranging from 0 to 4096 in (b) is the dynamic range of the digital camera. Over a good fraction of this dynamic range, the measured fractal dimension is essentially independent of the threshold. Figure 3c shows the scaling range in decades for each threshold. For the Reynolds numbers typical of most experiments in present series (about 5000 based on the nozzle diameter and velocity), the typical large/small scale ratio is about 100. Different symbols in (b) and (c) correspond to different realizations.

a plane, the above statement implies that the dimension of the intersected set is one less than the dimension of F.

The results so far have shown that the fractal dimension of the boundary in longitudinal (that is, streamwise) as well as orthogonal sections of prototypical fluid

Figure 4
A thin axial section of the scalar-marked region in the wake of a circular cylinder. The cylinder Reynolds number is about 1500.

flows is 1.35. It then follows that the fractal dimension of the surface is one greater than 1.35, or $D = 2.35$.

It may be useful to expand briefly on the result that the fractal dimension of intersections is independent of the orientation of the intersecting plane. While this result can be expected intuitively to be valid for fractally isotropic objects, flows considered here do have a preferential direction. We should, however, emphasize two points: First, the possible anisotropic properties of the interface will be confined essentially to the largest scales in the flow, these being on the order of the flow width (and larger). Secondly, the smaller scales for which fractal-like behaviour has been found are expected to be more or less isotropic, thus explaining our observation. Although we have been unable to take simultaneous orthogonal sections, experiments with independent sections have shown that the anisotropy effect may determine the precise range of scale similarity in two orthogonal planes but not the fractal dimension itself.

The principle of additive codimensions also implies that the fractal dimension of line intersections is two less than that of the surface; again, we have an opportunity

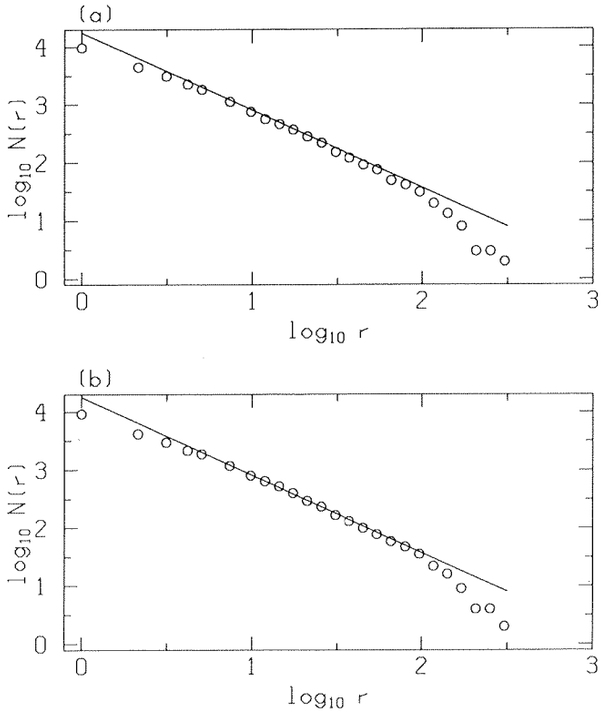

Figure 5
Results from the application of box counting methods to two orthogonal sections of a fully developed countercurrent mixing layer at a moderate Reynolds number; (a) plan view; (b) side view. For both of these sections, the slope of the straight lines is nominally the same, giving the fractal dimension of the boundaries to be 1.34.

Table 1

Table summarizing the fractal dimension measurements of scalar interfaces in four classical turbulent flows. There are marginal differences among the results in these flows, but the variability from one realization to another does not warrant any significance to be attached to these differences. We may conclude that the mean value is about 1.35

Flow	Fractal dimension of plane intersection of interfaces
axisymmetric jet	1.36*
boundary layer	1.36**
mixing layer	1.34#
plane wake	1.35*

*Average over a number of realizations (of the order 20) covering a streamwise extent of 5 to 30 diameters from the nozzle.
**Single value in the outer region.
#Average over a number of realizations (of the order 10) covering approximately a streamwise extent of two large structures.

here for testing the independence of the fractal dimension on the orientation of the intersecting line. By using box counting methods as before, one can compute the fractal dimension of the set of discrete points corresponding to the intersection of the interface by a given line (see Figure 2 for examples). Figure 6 shows the measured fractal dimension of some representative intersections (horizontal as well as vertical) as a function of the location of the section. Figure 7 shows that the results from line-cuts of arbitrary orientation are also the same. The mean values of D are not far from 2.35. (We have already made use of the additive principle.)

Equivalently, if one assumes that the flow is frozen (TAYLOR, 1938), one can take line intersection by fixing a point probe in the Eulerian frame and letting the flow convect past it. There is no reason to think that this will be accurate at all scales, but the hypothesis has been known to work roughly in a variety of

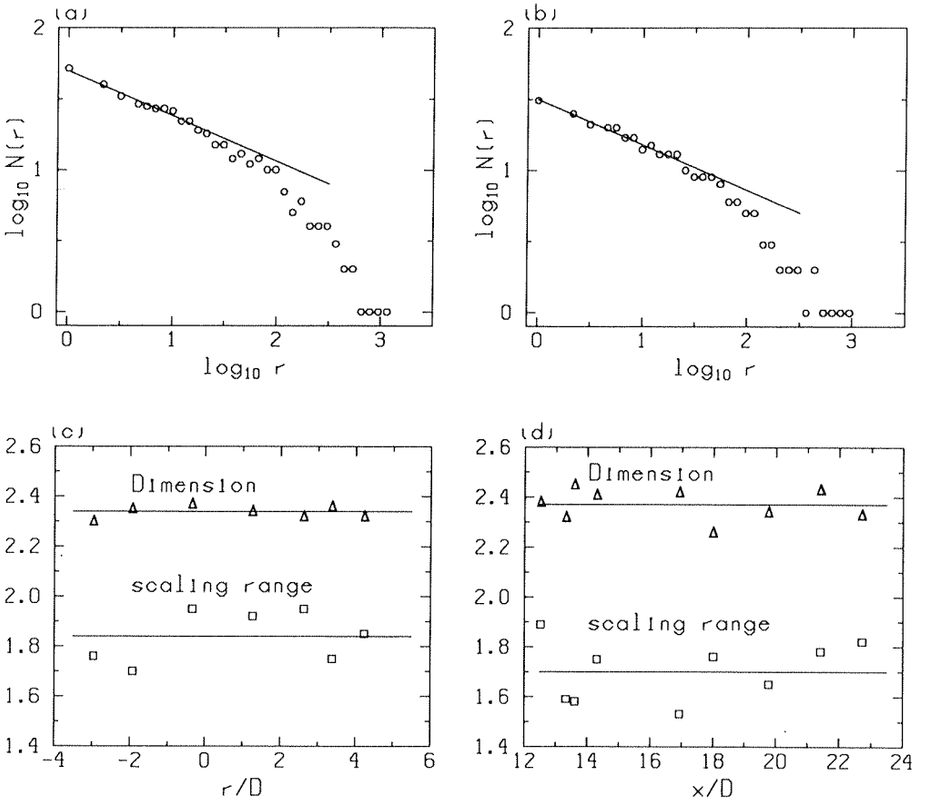

Figure 6
Typical results from one-dimensional cuts; (a) vertical and (b) horizontal, both referred to Figure 2. (c) and (d) indicate typical variability of the inferred D and the scaling range (in figures such as (a) and (b)) as a function of the position of the one-dimensional cut. The vertical cuts in (c) range from three diameters to the left of the axis to three diameters to the right. The horizontal cuts in (d) vary from 12 to 23 diameters downstream of the nozzle.

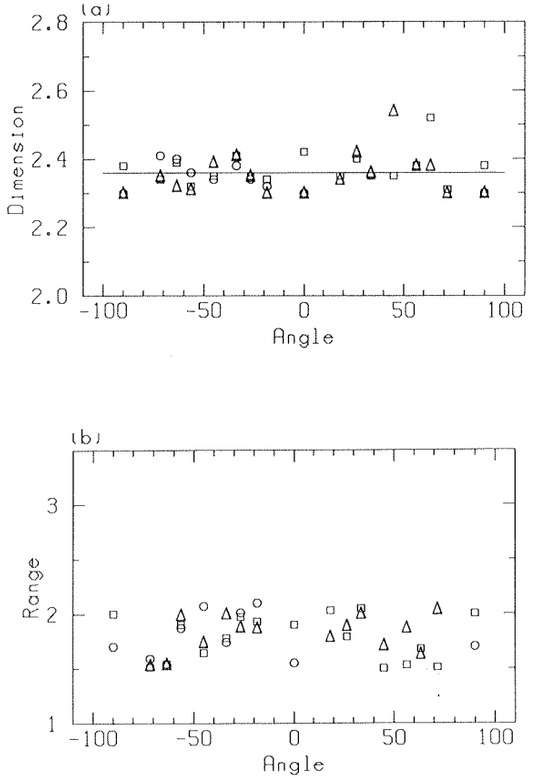

Figure 7
(a) Typical results from one-dimensional cuts passing through a fixed point as a function of the orientation of the intersecting line. Different symbols correspond to line cuts passing through different points. Figure (b) indicates the observed scaling range.

circumstances. We have used this approach also, and obtained results (Figure 8) for the nozzle fluid interface in a heated jet. Again, the inferred interface dimension has a mean value of 2.35, with the standard deviation on either side of about 0.05.

The last set of results obtained by the use of Taylor's frozen flow hypothesis are important because they enable us to conclude that the fractal dimension of scalar interfaces is independent of the mass diffusivity of the scalar: The dye and heat diffuse at rates which differ by about three orders of magnitude. Furthermore, the technique allows simple measurement of the fractal dimension of the vorticity interface as well. This has been discussed in I, where it was shown that the fractal dimension of this surface is also about 2.35.

We now have a very general result. To within the accuracy of measurement, the fractal dimension of vorticity and scalar interfaces (considering only scales

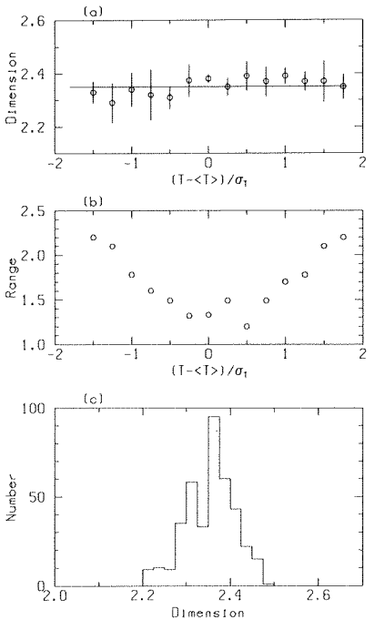

Figure 8
Fractal dimensions obtained by one-dimensional cuts using Taylor's frozen flow hypothesis in heated jets. (a) illustrates the constancy of the dimension with respect to the threshold, while (b) indicates the scaling range. In both (a) and (b), $\langle T \rangle$ is the mean temperature at the location of the measuring probe (a cold wire operated at 0.1 mA in the constant current mode), and σ is the root-mean-square fluctuation. Figure (c) is the histogram of D constructed using 390 realizations; the mean value is 2.35.

above η) in a number of fully developed turbulent flows, obtained by plane and line intersection techniques (whose validity we have established by a variety of measurements), is about 2.35. Clearly, the generality of the result demands an interpretation based on broad considerations. This is attempted in the next section.

3. *Mixing and Reynolds Number Similarity*

Let us consider transport by diffusion across interfaces of the type discussed so far. The flux is given by the product of the surface area, the concentration gradient normal to the surface and the molecular diffusivity. For fractals, the surface area S increases with the resolution of measurement r according to the relation (MANDELBROT, 1982)

$$S \sim r^{2-D}. \tag{1}$$

In all practical circumstances, the scale range over which (1) holds is bounded by cut-offs on both ends. For surfaces in turbulent flows, the outer cut-off is expected to occur at scales comparable to the integral scale, L, of turbulence, while the inner cut-off occurs at the smallest dynamical scale. For vorticity interfaces, the appropriate inner scale is the Kolmogorov scale $\eta = (\nu^3 \langle \varepsilon \rangle)^{1/4}$, where $\langle \varepsilon \rangle$ is the average rate of the turbulent energy dissipation. For with Schmidt number greater than unity, the relevant inner cut-off occurs at the Batchelor scale, $\eta_b = \eta\ Sc^{-1/2}$. The existence of a finite inner cut-off means that, as the surface area gets measured by covering it with increasingly finer area elements, a point is reached at which convolutions of even finer scales no longer exist, so that, thereafter, the area does not increase with increasing fineness of resolution; instead, it will saturate (abruptly in an ideal situation) at the maximum value corresponding essentially to the inner cut-off. The true area S_T of a fractal surface with finite inner cut-off is thus given (to within a constant) by the knowledge of the fractal dimension, and the inner cut-off r_i which theoretically truncates the power-law behaviour. Thus,

$$S_T = S_0 (r_i/L)^{2-D} \tag{2}$$

where S_0 is some normalizing area. If the area levels off at L and beyond, S_0 becomes the surface area measured with the resolution equal to L. It was also shown in III that for the case of high Schmidt numbers, it is natural to assume (in analogy with the inertial and viscous-convective ranges in the power-spectral density of passive scalar fluctuations) that there are two scaling regimes for the area S. In the range $\eta < r < L$, the relevant exponent is D, whereas in the range $\eta_b < r < \eta$, the relevant exponent will be designated D' and equation (2) is modified accordingly (see III).

It was shown in III that the characteristic velocity and concentration gradient across interfaces are of the order U_c/η and $\Delta C/\eta_b$, respectively. U_c is a characteristic velocity, for example the centerline defect velocity for the wakes, the centerline excess velocity for the jets, the velocity difference between the two streams for the mixing layer, and the friction velocity (equal in kinematic units to the square root of the wall shear stress) for the boundary layer. ΔC is a characteristic concentration difference.

From these considerations, an expression for the flux of momentum across the interface can be written as

$$\nu S_T (U_c/\eta). \tag{3}$$

Defining the characteristic Reynolds number $\mathrm{Re} = u'L/\nu$ (u' being the root-mean-square of the velocity fluctuations), we may note that $\eta/L \sim \mathrm{Re}^{-3/4}$, and use equation (2) for the interface area S_T to write (after a little algebra) that the

$$\text{flux of momentum} \sim S_0 U_c^2 (u'/U_c)\ \mathrm{Re}^{3(D-7/3)/4}. \tag{4}$$

Note that S_0, U_c and (u'/U_c) are all independent of Reynolds number. For nonunity Schmidt numbers, the corresponding result for the flux of a species with concentration difference ΔC is given by

$$\text{flux of contaminant} \sim S_0 (U_c \cdot \Delta C)(u'/U_c)\ \mathrm{Re}^{3(D-7/3)/4} Sc^{\gamma}, \tag{5}$$

where $\gamma = 0.5\ (D' - 3)$ for $Sc > 1$ and $\gamma = 3\ (D - 7/3)/4$ for $Sc < 1$.

Now, it is well-known that all fluxes (mass, momentum, energy) must be independent of Reynolds number in fully turbulent flows—the so-called Reynolds number similarity. (This is merely a statement of the observed fact that the growth rates of turbulent flows of a given configuration are independent of fluid viscosity.) According to (4) and (5) the Reynolds number similarity requires that

$$D = 7/3, \tag{6}$$

for both the vorticity and scalar interfaces, in rough agreement with experiments (see Table 1). Since the fluxes are expected to be also independent of Sc (the so-called Schmidt number similarity), equation (5) implies that $\gamma = 0$, or $D' = 3$. This means that the convolutions of the interface on scales between η_b and η are essentially space-filling.

In the above arguments we have assumed that it is appropriate to use a common characteristic velocity or concentration gradient everywhere along the interface. This is not strictly true, at least because the interface thickness varies from place to place because of the spatial intermittency of the dissipation rate ε (see Section 4). Furthermore, it is implied above that the globally averaged dissipation rate is the same as that averaged in the neighborhood of the interface alone. These two limitations were addressed in detail in III, where it was shown that the intermittent nature of the dissipation near the interface is statistically the same as that elsewhere, and that the inclusion of the intermittency will alter D from 7/3 to 2.36. This latter estimate is in excellent agreement with our experimentally determined mean value of 2.35. It is worth mentioning that the reason for the relatively small correction is that the interface thickness depends on the quarter power of the dissipation, and so the strong variabilities in ε do not translate to comparable variations in the interface thickness.

4. *The Multifractal Distributions of Dissipation Rates of Turbulent Kinetic Energy and Passive Scalar Fluctations*

There has been an explosive interest in recent years in the characterization of measures created by multiplicative processes. Starting with MANDELBROT (1974), several formalisms have been introduced (HENTSCHEL and PROCACCIA, 1983; FRISCH and PARISI, 1985; HALSEY *et al.*, 1986; MANDELBROT, 1988). In turbulence,

the transfer of kinetic energy from the large scales of motion to the smaller scales can be thought of as arising from a multiplicative cascade process. Therefore, the manifestation of this flux at the smallest scales, which is the dissipation ε, is expected to be a multifractal. The same can be said for the flux of the variance of a passive scalar and its dissipation χ. In such a description, the total dissipation of kinetic energy E_r that is contained in a box of size r obeys a local power law

$$E_r \sim r^{\alpha}, \tag{7}$$

where α varies from point to point. A similar power-law is expected to hold for X_r, the amount of χ in a box of size r. Since the values of α for the scalars need not be the same as those for the energy, the notation in (7) is to be regarded as generic. The number of boxes with α within in a band $d\alpha$ is assumed to scale according to

$$N(\alpha)\, d\alpha \sim r^{-f(\alpha)}\, d\alpha. \tag{8}$$

As one covers the measure with boxes of decreasing size, the number of occurrences of a certain α generally increases (that is, $f(\alpha) > 0$), or remains constant (that is, $f(\alpha) = 0$). In such cases, $f(\alpha)$ is interpreted as the fractal dimension of iso-α sets. (For a more detailed discussion of this point, see CHHABRA *et al.*, 1989.) MANDELBROT (1988) has shown that cases exist for which $f(\alpha)$ is negative; we will return to this point below.

A dual description of multifractals is given in terms of the q-moments of E_r and X_r; in that case one measures the 'generalized box dimensions' (HENTSCHEL and PROCACCIA, 1983), $D_q(\varepsilon)$ and $D_q(\chi)$ of ε and χ respectively, defined as

$$\Sigma E_r \sim r^{(q-1)D_q(\varepsilon)}, \quad \text{and} \quad \Sigma X_r \sim r^{(q-1)Dq(\chi)}. \tag{9}$$

The quantities $f(\alpha)$ and α are then obtained by the well-known Legendre transforms (HALSEY *et al.*, 1986)

$$\alpha = d/dq[(q-1)D_q] \quad \text{and} \quad f(\alpha) = q\alpha - (q-1)D_q. \tag{10}$$

Although $f(\alpha)$ can be determined directly, MENEVEAU and SREENIVASAN (1989) have shown that it is more practical to obtain them by first measuring the D_q exponents and using (10). This is due to second-order finite-size corrections to $N(\alpha)$ that appear in (8), which are important in experimental situations at moderate Reynolds numbers.

Measurements of the D_q curve from one-dimensional cuts through ε were reported in II, and the corresponding curves for the dissipation of passive scalar fluctuations from one- and two-dimensional intersections were reported in IV. The $f(\alpha)$ curves obtained by the use of (10) are shown in Figures 9a,b. (For readers

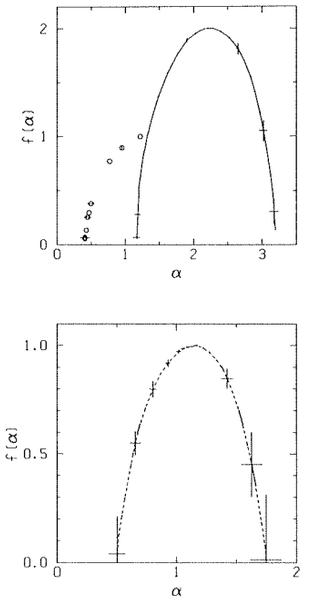

Figure 9

$f(\alpha)$ curves of lower-dimensional sections through the dissipation fields. (a) Dissipation of passive scalar fluctuations: The continuous line represents the mean results from two-dimensional measurements of concentration (a passive scalar) in water jets (see IV). Circles correspond to one-dimensional measurements of temperature (also a passive scalar) in heated air jets. Since there are some experimental difficulties associated with the determination of the D_q's for $q < 0$ in the one-dimensional sections (see IV), only the left half of the curve is shown. (b) Dissipation of kinetic energy: The dashed line corresponds to the average $f(\alpha)$ curve for one-dimensional sections in several fully developed turbulent flows (see II). In both figures, bars show the variability in measurements.

familiar with our earlier work, it is useful to note a change of notation. In II and IV, α was defined in terms of the average dissipation on a domain r according to $\varepsilon_r \sim r^{\alpha-1}$ for any dimensionality of the box. Here, we use equation (7) as the basic definition and therefore $\varepsilon_r \sim r^{\alpha-d}$, where d is the dimensionality of the domain in which the dissipation is embedded: d is 1 for one-dimensional cuts, 2 for planar intersections and 3 for the case in three dimensions.)

Several properties of the lower-dimensional intersections can now be discussed. We shall assume here, and defer questions of exceptions to a later stage, that the additive properties of fractal dimensions discussed in Section 2 hold also for $f(\alpha)$; that is, $f(\alpha)$ in three-dimensional space can be obtained by adding 2 to that obtained by linear cuts and by adding 1 to the results from planar cuts. Similar additive properties hold for α, since lower-dimensional cuts measure densities that can be

integrated over boxes of different dimensionalities (for details see MANDELBROT, 1988). Figure 10 shows the $f(\alpha)$ curves of ε and χ obtained by translating according to the above additive law the values of α and $f(\alpha)$ of Figure 9. It is apparent that the $f(\alpha)$ curve for χ is wider than that for ε; as discussed in IV, this is consistent with the well-known result that the dissipation of passive scalar is more intermittent than the energy dissipation.

The $f(\alpha)$ curve of ε obtained for one-dimensional cuts was modeled in MENEVEAU and SREENIVASAN (1987b) by a two-scale Cantor measure (the p-model). In order to reproduce the experimental observations, the following three-dimensional cascade process was proposed: After every step of the cascade, each eddy splits into 2^3 smaller eddies. Half of them each receive a fraction $p_1/4 = 0.7/4$ of the energy flux, while each of the others receive the remaining fraction $p_2/4 = 0.3/4$. As pointed out in SREENIVASAN and MENEVEAU (1988), this would imply that there are no singularities with $f(\alpha) < 2$, but this can be corrected by perturbing the p-model slightly and assuming that each eddy receives a fraction $p_1/4 \pm \delta$ or $p_2/4 \pm \delta$, where

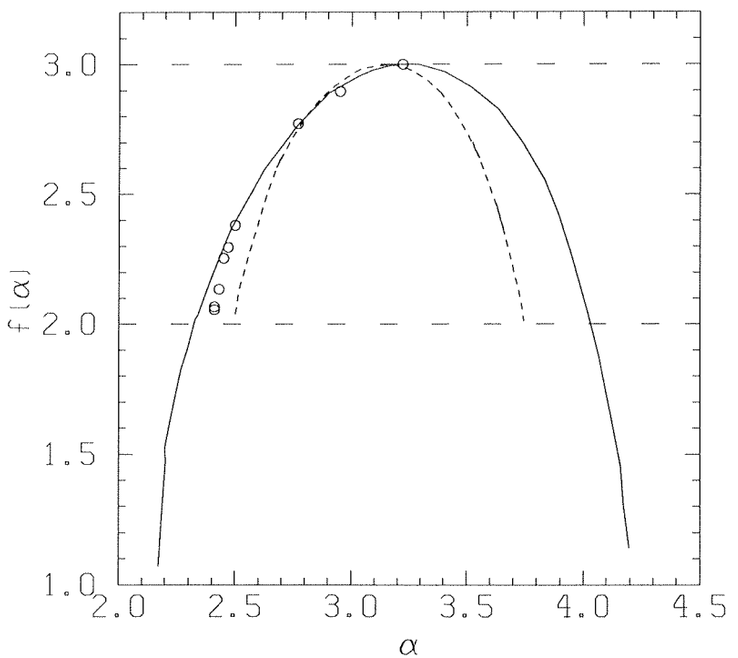

Figure 10

$f(\alpha)$ curves of lower-dimensional sections through the dissipation fields, translated in such a way as to correspond to the situation in three-dimensional space. Symbols as in Figure 9. Where they overlap, the passive scalar data obtained from one and two-dimensional sections agree well. The figure also shows that the $f(\alpha)$ curve for the scalar dissipation curve is wider than that for the energy dissipation.

δ is different for each eddy (MENEVEAU, 1989). Obviously, these perturbations are subject to the overall conservation of the energy flux.

We now discuss an issue raised by MANDELBROT (1988). By necessity, the discussion here is very brief, and will be expanded elsewhere using appropriate experimental evidence. The issue is the use of lower-dimensional cuts to obtain information on *very sparse* sets of singularities, whose $f(\alpha)$ in three dimensions is less than the co-dimension of the intersecting subspace. MANDELBROT (1988) has shown that this is in principle a valid procedure, provided that averages are performed over regions that are much larger than the integral scale of the flow. He has further shown (see also MANDELBROT, 1974) that if the energy cascade proceeds in such a way that a sub-eddy receives an amount of energy that is higher than a certain fraction, the implication is that lower-dimensional cuts would show negative values of α and D_q's for $q > q_{cr}$. It follows that a possible criticism of the measurements reported above is that, since only the last step of the cascade is accessible in measurements, negative values of α and D_q (if they exist) are impossible to detect, and therefore D_q's for $q > q_{cr}$ may have been biased.

If one extrapolates the curves of Figure 9a down to $f(\alpha) = 0$, it appears that α is always larger than 2 (especially for the energy dissipation), suggesting that no negative α's are present even in one-dimensional cuts. The question now concerns the reliability of the $f(\alpha)$ curves in Figure 9 especially near the tails (which are determined by high order D_q's—both positive and negative), as well as the extrapolation procedure. We point out that the positive part of the $f(\alpha)$ curve from lower-dimensional cuts can be obtained more or less completely using values of q up to about 6. An indication that D_q's for q values of that order are quite accurate comes from the agreement of our results with those inferred from other experiments (ANSELMET *et al.*, 1984) in that range of q. From this and further evidence to be reported in the near future, we conclude that D_q's at least up to order 6 are not biased, and, therefore, that there are no negative α's. If this is so, then the cascade proceeds without ever surpassing the limit on the fluxes mentioned above, this being a very strong statement about the physics of the cascade. One can get an idea of this limit by using the three-dimensional p-model, for which this limit is 1/4.

At any rate, the quantification of a multiplicative measure by $f(\alpha)$ is degenerate at many levels (FEIGENBAUM, 1987; MANDELBROT, 1988; CHHABRA *et al.*, 1989), and it is not clear how much of the underlying physics can be extracted unambiguously from such a description.

Acknowledgements

We are thankful for financial support to the Air Force Office of Scientific Research (which supported the initial phases of this work) and the Defence Advanced Research Projects Agency (which has sustained the later phases).

REFERENCES

ANSELMET, F., GAGNE, Y., HOPFINGER, E. J., and ANTONIA, R. A. (1984), *High-order Velocity Structure Functions in Turbulent Shear Flows*, J. Fluid Mech. *140*, 63.

CHHABRA, A., JENSEN, R., and SREENIVASAN, K. R. (1989), *Multifractals, Multiplicative Processes and the Thermodynamic Formalism*, Phys. Rev. A (in print).

FEIGENBAUM, M. (1987), *Some Characterizations of Strange Sets*, J. Stat. Phys. *46*, 919.

FRISCH, U., and PARISI, G., *On the singularity structure of fully developed turbulence*, In *Turbulence and Predictability in Geophysical Fluid Dynamics and Climate Dynamics* (eds. Ghil, M., Benzi, R., and Parisi, G.) (North-Holland, New York 1985).

HALSEY, T. C., JENSEN, M. H., KADANOFF, L. P., PROCACCIA, I., and SHRAIMAN, B. I. (1986), *Fractal Measures and their Singularities: The Characterization of Strange Sets*, Phys. Rev. *A33*, 1141.

HENTSCHEL, H. G. E., and PROCACCIA, I. (1983), *The Infinite Number of Generalized Dimensions of Fractals and Strange Attractors*, Physica *8D*, 435.

MANDELBROT, B. B. (1974), *Intermittent Turbulence in Self-similar Cascades: Divergence of High Moments and Dimension of the Carrier*, J. Fluid Mech. *62*, 331.

MANDELBROT, B. B., *The Fractal Geometry of Nature* (Freeman, San Francisco 1982).

MANDLEBROT, B. B., *An introduction to multifractal distribution functions*, In *Fluctuations and Pattern Formation* (eds. Stanley, H. E., and Ostrowsky, N.) (Kluwer, Dordrecht-Boston 1988); see also this volume.

MARSTRAND, J. M. (1954), *Some Fundamental Geometrical Properties of Plane Sets of Fractal Dimensions*, London Math. Soc. *3*, 257.

MATTILA, P. (1975), *Hausdorff Dimension, Orthogonal Projections and Intersections with Planes*, Ann. Acad. Sci. Fenn. Ser. A I Math. *1*, 227.

MENEVEAU, C. (1989), *The Multifractal Nature of Turbulence*, Ph.D. Thesis, Yale University.

MENEVEAU, C., and SREENIVASAN, K. R. (1987a), *The Multifractal Dissipation Field in Turbulent Flows*, Nuclear Physics B (Proc. Suppl.) *2*, 49.

MENEVEAU, C., and SREENIVASAN, K. R. (1987b), *Simple Multifractal Cascade Model for Fully Developed Turbulence*, Phys. Rev. Lett. *59*, 1424.

MENEVEAU, C., and SREENIVASAN, K. R. (1989), *Measurement of $f(\alpha)$ from Scaling of Histograms, and Application to Dynamical Systems and Fully Developed Turbulence*, Phys. Lett. A (in print).

PRASAD, R. R., MENEVEAU, C., and SREENIVASAN, K. R. (1988), *Multifractal Nature of the Dissipation Field of Passive Scalars in Fully Turbulent Flows*, Phys. Rev. Lett. *61*, 74.

PRASAD, R. R., and SREENIVASAN, K. R. (1989), *Scalar Interfaces in Digital Images of Turbulent Flows*, Experiments in Fluids *7*, 259.

RAMSHANKAR, R. (1988), *The Dynamics of Countercurrent Mixing Layers*, Ph.D. Thesis, Yale University.

RICHARDSON, L. F., *Weather Prediction by Numerical Process* (Cambridge University Press, Cambridge, U.K. 1922).

SREENIVASAN, K. R., and MENEVEAU, C. (1986), *The Fractal Facets of Turbulence*, J. Fluid Mech. *173*, 357.

SREENIVASAN, K. R., and MENEVEAU, C. (1988), *Singularities of the Equations of Fluid Motion*, Phys. Rev. *A38*, 6287.

SREENIVASAN, K. R., RAMSHANKAR, R., and MENEVEAU, C. (1989), *Mixing, Entrainment, and Fractal Dimension of Interfaces in Turbulent Flows*, Proc. Roy. Soc. Lond. *A421*, 79.

TAYLOR, G. I. (1938), *The Spectrum of Turbulence*, Proc. Roy. Soc. Lond. *A164*, 476.

(Received September 14, 1987, revised/accepted June 1, 1988)